



Theoretical Study for Chemical Reactivity of Diuron

¹R.Tazi, ²H.El Hadki, ³M.Salah, ⁴S.Izzaouiha, ⁵N.Komiha

¹Laboratory of Materials, Nanomaterials and Environment, Faculty of Sciences, Mohammed V University, Rabat, Morocco

^{2,3,4,5}Laboratory of Spectroscopy, Molecular Modeling, Materials and Environment, Faculty of Sciences, Mohammed V University, Rabat, Morocco

DOI: [10.23956/ijarcse/SV715/0162](https://doi.org/10.23956/ijarcse/SV715/0162)

Abstract: *A theoretical study of 3-(3,4-dichlorophenyl)-1,1-dimethyl urea and protonated forms are specified to rationalize experimental results on electrostatic interactions in the herbicide models, to describe structural changes taking place between gaseous and aqueous solution. It was found that its multibasic structures suggests us three sites of protonation. Calculations have been performed on neutral and protonated forms using DFT with functional B3LYP. Characterization of electronic parameters and molecular density has been studied. To determine the reactive sites, we are interested in the local and global reactivity descriptors analyzing the molecular reactivity. The calculations have shown that attacks on the unsubstituted core positions are preferred to those of the aromatic ring. The study of the effect of the solvent has revealed a particularly sensitive to electrostatic environment. The calculated vibrational normal modes have been assigned on the basis of literature spectroscopic data.*

Keywords: *Quantum chemical calculations; Diuron; Protonation; Global reactivity descriptors; Solvation.*

I. INTRODUCTION

Pesticides are commonly used in agricultural areas; their extensive use causes pollution of soil and aquatic ecosystems. Among these chemicals, Diuron ($C_9H_{10}Cl_2N_2O$), (Figure 1), herbicide dimethyl substituted by chlorine atoms belongs to the family of the substituted ureas. It is widely applied for the control of annual grasses and weeds in many crops[1]. It is also used as antimould in the paintings, algacide in ponds and aquariums as well as identified in water courses. Diuron is a significant pollutant, has a toxic effect on plant photosynthesis, is considered dangerous for aquatic life and flora and presents considerable potential which is the cause of congenital defects for humans[2–10]. As a result, it has been classified as a carcinogen since 1997. Diuron is considered persistent (half life in soil more than 360 days), very noxious and harmful to the human body[11–13]. When it is widespread in the environment, only a small proportion reaches its objective but surplus enters the ground, water or air[14]. For these agronomic and environmental aims, it is important to have information on this organic complex that takes place in contact with the ground. As its action depends largely on the quantity of water that moves and on the retention time in the soil; it is interesting to determine it in aqueous solution. In the present work, diverse paths of protonation of Diuron are studied using density functional theory (DFT). We realized a geometry optimization, a simulation of the attack on different atoms of the exocyclic chain of Diuron, a determination of the reactive sites, analysis and allocation of normal modes of vibration then the effect of solvation.

II. MATERIALS AND METHODS

Neutral and protonated Diuron study has knowledgeable an important development for its applications in various chemical problems[15–18]. With the functional theory of the density (DFT), we optimize the geometry of the molecule; predict the chemical properties, dipole moments and frontier molecular orbitals. The functional hybrid B3LYP[19–22] coupled by the 6-311G++ (d,p) basis with the Gaussian03 software[23] was used without any restriction of symmetry. All calculations converged at 10⁻⁸ u.a. The frequency calculation was carried out to verify the stable configuration of each optimized structure using the same base to obtain the zero point vibrational energy (ZPVE), assigned and compared with the experimental values. No imaginary frequencies were obtained confirming that the stationary point corresponds to a minimum of the potential energy surface. The determination of the reactive sites of the compound was carried out by analyzing the local indices and the overall reactivity parameters derived from the functional theory of density. The spectroscopic study allowed us to determine the absorption vibrational bands. The gap between the theoretical and experimental spectroscopic values is generally due to scale factor. The algorithm that deals with this kind of error is not employed in Gaussian03, consequently vibrational frequencies have been determined analytically to geometry fully optimized and scaled by a factor 0.9804 to correct the vibrational anharmonicities[24,25] (determined as the average value of the ratio of theoretical/experimental wave numbers). All the geometries of the calculated electronic structures have been built and viewed using the graphical interface GaussView[26]. To take account of the solvent effects, we used the PCM polarizable continuum model[27,28] with the dielectric constant 78.5 for water at 298.15 °K and 1 atm.

III. RESULTS AND DISCUSSION

A. Structure

The Diuron was optimized at the B3LYP/6-311++G (d,p) level in the gas phase and this last structure was used as starting point to reoptimize it without any symmetry constraints employing the PCM model to take into account the effect of solvation. The geometrical parameters of the optimized structure of neutral Diuron reported in figure 1, C₁ symmetry, as well as the experimental parameters determined from an RX (values in parentheses)[29] analysis are reported in table 1.



Fig.1. Structure of Diuron 3-(3, 4-dichlorophenyl) 1,1dimethylurea)

Table 1 Calculated and experimental structural parameters of Diuron

BOND DISTANCES IN Å		VALENCE ANGLES IN °		DIHEDRAL ANGLES IN °	
C3C2	1,389 (1,383)	C2C3C4	120,56 (121,1)	C4C3C2C1	0,00
C3C4	1,390 (1,365)	C2C3C1	117,83	C4C3C2H1	-180,00
C3C11	1,818 (1,770)	C4C3C11	121,62	C11C3C2C1	-180,00
C2C1	1,406 (1,389)	C3C2C1	118,93 (118,0)	C11C3C2H1	0,00
C2H1	1,081 (0,960)	C3C2H1	118,93 (120,0)	C2C3C4C5	0,0
C1C6	1,406 (1,365)	C1C2H1	120,62	C2C3C4C12	-180,0
C1N1	1,411 (1,326)	C2C1C6	119,03 (122,2)	C11C3CC5	180,0
C6C5	1,393 (1,394)	C2C1N1	116,92	C11C3C4C1	0,00
C6H3	1,076 (1,050)	C6C1N1	124,05 (121,0)	C3C2C1C6	0,00
C5C4	1,393 (1,380)	C1C6C5	119,58 (118,4)	C3C2C1N1	180,00 (176,8)
C5H2	1,080 (1,060)	C1C6H3	119,47 (118,0)	H1C2C1C6	180,00
C4C12	1,816 (1,770)	C5C6H3	120,95 (114,0)	H1C2C1N1	0,00
N1H4	1,005 (0,890)	C6C5C4	121,16 (120,3)	C2C1C6C5	0,00
N1C7	1,396 (1,375)	C6C5H2	119,66	C2C1C6H3	180,00
C7N2	1,381 (1,326)	C4C5H2	119,18	N1C1C6C5	-180,00
C7O1	1,254 (1,245)	C3C4C5	119,22 (120,0)	N1C1C6H3	-0,00(-0,06)
N2C8	1,465 (1,470)	C3C4C12	121,87	C2C1N1H4	-0,00
N2C9	1,468 (1,470)	C5C4C12	118,91	C2C1N1H4	-180,00
C8C8	1,095 (1,090)	C1N1H4	114,76 (120,0)	C6C1N1H4	180,00
C8H6	1,087 (1,090)	C1N1C7	127,34 (124,4)	C6C1N1C7	0,00 (28,3)
C8H7	1,095 (1,090)	H4N1C7	117,89	C1C6C5C4	0,0
C9H8	1,092 (1,090)	N1C7N2	115,05 (115,0)	C1C6C5H2	180,00
C9H9	1,092 (1,090)	N1C7O1	122,53 (122,6)	C6C5C4C3	-0,00
C9H10	1,085 (1,090)	N2C7O1	122,42	C6C5C4C12	180,00
		C7N2C8	123,61	H2C5C4C3	-180,00
		C7N2C9	118,35	H2C5C4C12	-0,00
		C8N2C9	118,04	C1N1C7N2	-180,00
		H5C8H6	107,28	C1N1C7O1	-0,00 (2,6)
		H5C8H7	109,15	H4N1C7N2	0,00
		H6C8H7	107,28	H4N1C7O1	-180,00
		N2C9H8	110,66	N1C7N2C8	-0,00

		N2C9H9	110,66	N1C7N2C9	-180,00
		N2C9H10	108,22	C7N2C8H6	180,00
		H8C9H9	109,03	C7N2C8H10	-61,63
		H8C9H10	109,12	C9N2C8H5	-118,36
		H9C9H10	109,12	C9N2C8H6	0,00
				C9N2C8H7	118,37
				C7N2C9H8	119,52
				C7N2C9H9	-119,52
				C7N2C9H10	0,00
				C8N2C9H8	-60,48
				C8N2C9H9	60,48
				C8N2C9H7	-180,00

The differences between the values are due to the fact that experimental data describe the solid state while calculations are performed on an isolated molecule. In the solid state, the molecule is not planar but presents a torsion angle of 48.2° around the N1-C1 binding, which is certainly due to intermolecular hydrogen bonds[30]. The calculated values of dihedral angles reveals that the molecular structure has a planar conformation with a partial electron delocalization between the substituted phenyl group and the dimethylurea of the molecule: angle is close to 180° and 0° for 28.3° and 2.6° experimentally. The aromatic ring C-C bond lengths are equivalent in order of 1.40 Å. Partial electron delocalization testifies to the sp² nature of the atom N1 forming three bonds almost planar with the C1N1C7, H4N1C7, C1N1H4 respectively 127°34', 117°89', 114°76' and so close to 120°. The atoms O1 and N2 don't seem to participate in this relocation. In fact, the C7-O1 bond length (1.254 Å) is shorter and the N2 atom has a pyramidal environment. From the electronic point of view, with regard to the N1 atom, this rotation gives the impression that the molecule is separate into two parts: on one side, there is the phenyl and on the other side there is a relocation action leading to a decrease of the C=O bond (from 1.254 to 1.245 Å) and C1-N1 (from 1,411 to 1,326 Å) as well as a character sp² for the atom N1. The bond distances and angles obtained at the B3LYP/6-311G++ (d,p) level are in good agreement with those reported in the literature[29–31]. A frequency analysis was applied to the optimized geometries to attest that the stationary points correspond to the minimum of the potential energy surface. In all cases, the frequencies values were positive and no imaginary frequency was obtained.

B. Charges and dipole moment

The calculation of point charges will allow us to confirm the sites of protonation for studied compound and to evaluate the electron density on each atom of Diuron. The Mulliken charges obtained are reported in table 2 (values in parentheses are for aqueous solution). Indeed, the determination of the atom which carries the negative charge will give us an indication on the direction of approach of the proton.

Table 2 Values of the charges determined by DFT calculations

$q_k(N)$					
C 1	-0.4112 (-0.7514)	C 9	-0.4831 (-0.5166)	H 3	0.1495 (0.2061)
C 2	-0.4370 (-0.1081)	N 1	-0.1780(-0.1315)	H 4	0.3908 (0.4288)
C 3	-0.3521 (-0.5642)	N 2	-0.0265(-0.0223)	H 5	0.1930 (0.1744)
C 4	0.5183 (0.4743)	O 1	-0.3571(-0.4612)	H 6	0.1503 (0.1728)
C 5	-0.0734 (0.0315)	Cl 1	0.4803(0.4345)	H 7	0.1630 (0.1744)
C 6	-1.1046 (-0.9405)	Cl 2	0.6196(0.5856)	H 8	0.1451 (0.1717)
C 7	0.0795 (0.0801)	H 1	0.2329(0.2215)	H 9	0.1845 (0.1998)
C 8	-0.2567 (-0.2698)	H 2	0.2153(0.2383)	H 10	0.1576 (0.1719)

The positive charge on the hydrogen atom from the NH group indicates its aptitude to form a hydrogen bond with a proton donor. The negative charge on the nitrogen and oxygen atoms specifies their ability to form a hydrogen bond with an acceptor. For that reason, it is concluded that these will be the highest points of contact. From these results, the protonation would be preferentially at the level of part urea and more particularly on the oxygen of the carbonyl group. We find the results obtained previously. With regard to the dipole moment μ , the values calculated in gaseous phase and aqueous phase are respectively 5.77 and 7.84 Debye. The structural study allowed us to show the geometric properties of Diuron and the assignment of protonation. The multibasic structure reveals that the protonation sites are three for Diuron so therefore three isomers were determined indicating the protonation on the exocyclic part of the molecule. The active sites of protonation O1, N1, N2 are indicated by arrows for the examination of an electrophilic attack (figure 2).

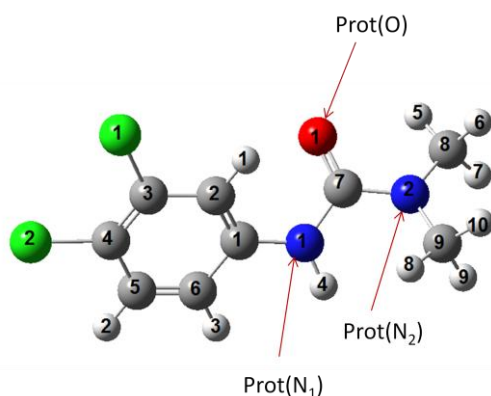


Fig. 2. Structure of Diuron and active sites of protonation

In table 3, it can be noticed that the protonation has no effect on the overall geometry of the pesticide but gives formation of a hydrogen bond by 0.980 Å and 1.026 Å.

Table 3 Calculated and experimental parameters of neutral and protonated Diuron

	DIURON			
	NEUTRAL (X RAY)	PROTONATED		
		O ₁ N ₁ N ₂		
N ₁ H ₄	1.010	1.014	1.030	1.013
N ₂ C ₇	1.383	1.325	1.336	1.568
C ₇ O ₁	1.232	1.325	1.229	1.226
N ₁ C ₇	1.396	1.347	1.588	1.344
O ₁ H	-	0.980	-	-
N ₁ H	-	-1.026	-	-
N ₂ H	-	--1.026	-	-
N ₂ C ₇ O ₁	122.76	117.45	131.39	116.06
N ₁ C ₇ N ₂	114.54	123.06	114.68	112.77
N ₁ C ₇ O ₁	122.70	119.49	113.93	131.17
HO ₁ C ₇	-	110.77	--	--
HN ₁ C ₇	-	-112.26	-	-
HN ₂ C ₇	-	--111.05	-	-
N ₁ C ₁ C ₆ H	-0.06	-0.74	0.14	0.13
H ₄ N ₁ C ₁ C ₂	0.04 (28.3)	2.20	0.30	0.03
C ₇ N ₁ C ₁ C ₆	179.99 (29.4)	130.88	130.98	0.04
O ₁ C ₇ N ₁ C ₁	-0.98 (2.6)	0.14	91.47	-0.04
N ₂ C ₇ N ₁ H ₄	-185.00 (0.5)	0.06	38.36	0.01
C ₈ N ₂ C ₇ N ₁	174.65 (-175.5)	179.92	-178.63	-
C ₉ N ₂ C ₇ O ₁	-176.09 (-	119.33		
N ₂ C ₇ O ₁ H	174.0)	-179.89	-0.78	-60.84
N ₁ C ₇ O ₁ H	-	179.95	--	--
	-	-0.06	--	--

The calculations, made at the same level of calculation, showed that solvation has no effect on the overall geometry of the studied compounds.

C. Energies and proton affinity

Initially, the energies were determined in the gas phase for the neutral compound and for the three protonated forms, then by introducing water as a solvent (values in parentheses). The effect of solvent was taken into account by a single calculation point on optimized gas phase geometries using the PCM (polarizable continuum Model) of Tomasi model [27]. The results are presented in table 4.

Table 4 Calculated energies at the B3LYP/6-311++G (d,p) level of theory in u.a

METHODS / BASE OF CALCULATION	E _T DIURON	E _T PROT(O)	E _T PROT(N ₁)	E _T PROT(N ₂)
DFT / B3LYP	-1454.320298	-1454.678719	-1454.651854	-1454.660283
6.311G++(d,p)	(-1454.332946)	(-1454.755398)	(-1454.738324)	(-1454.752188)

The results obtained allow us to characterize the preferential protonation site. It may be noted that the protonated forms are energetically promoted. As we can see in the above results, the position of the carbonyl group of the urea (prot(O)) function has stabilized; this is the most favourable site for protonation. We know that the Born-Oppenheimer approximation gives a lower energy than the real energy of the system because the nuclear movements are neglected; the energy obtained must be corrected to the zero point absolute. Thus the proton affinity (PA) is resolved by the relationship:

$$PA (M) = [E (M) - E (MH^+)] + [ZPE (M) - ZPE (MH^+)]$$

where (M) represents the neutral form and (MH⁺) the protonated form.

Table 5 Proton affinity of neutral and protonated Diuron for 6-311G++ (d, p)

	ZPE (u.a)	PA (Kcal/mol)
DIURON	0.194930 (0.194846)	- -
DIURON PROT (O)	0.207804 (0.207693)	216.83 (257.03)
DIURON PROT (N ₁)	0.208530 (0.208617)	199.52 (245.73)
DIURON PROT (N ₂)	0.208874 (0.209547)	204.59 (253.85)

The results obtained in the table 5 show that the protonation at the level of the O atom is more favourable than on N1 and N2 with an energy gap of 17.3 and 12.2 Kcal/mol respectively by introducing the system energy absolute zero (ZPE). Taking into account the effect of solvent reduces this difference to 11.3 and 3.2 Kcal/mol. In the two conditions, the hierarchy of the values of PA is respected in the protonated forms:

$$PA (\text{prot (O)}) > PA (\text{prot (N}_2\text{)}) > PA (\text{prot (N}_1\text{)})$$

D. Charges and dipole moment of protonated Diuron

The calculation of point charges have been performed to evaluate the electron density of studied compound and will let us confirm the sites of protonation for studied compound. The results obtained are reported in table 6.

Table 6 Values of the charges determined by DFT calculations

$q_k(N)$	DIURON NEUTRAL	DIURON PROTONATED		
		O ₁	N ₁	N ₂
q H ₄	0.3908 (0.4288)	0.3772 (0.4064)	0.3065 (0.3458)	0.2393 (0.2816)
q N ₁	-0.1780 (-0.1315)	0.0462 (0.1299)	-0.0180 (0.0339)	0.0384 (0.0559)
q N ₂	-0.0265 (-0.0223)	-0.0458 (-0.0057)	0.0056 (0.0522)	-0.2721 (-0.1941)
q O ₁	-0.3571 (-0.4612)	-0.2120 (-0.2416)	-0.2137 (-0.2888)	-0.2412 (-0.3084)
q C ₇	0.0795 (0.0801)	0.0384 (0.0292)	-0.5410 (0.0254)	-0.7630 (-0.8243)
q H	-	0.3735 (0.392010)	0.3861 (0.4120)	0.3929 (0.4150)

Mulliken charges on the three exocyclic sites of protonation, highest points of contact, have values between -0.02 and -0.46 in aqueous medium. From these results, the protonation would be preferentially at the level of part urea and more particularly on the oxygen of the carbonyl group. We find the results obtained previously.

With regard to the dipole moment μ , the values calculated in gaseous phase and aqueous phase are presented in table 7.

Table 7 Values of the dipole moments

μ (Debye)	Diuron prot(N ₂)	prot(O ₁)	prot(N ₁)
DFT / B3LYP 6.311G++(d,p)	5.774 16.700 (7.841) (20.355)	11.441 (13.993)	12.585 (15.962)

The values obtained show an increase for the solvated form so an ability to bind or connect a strongly polar site.

E. Frontier orbitals

The HOMO-LUMO energy gap is a significant indication of stability. Indeed, a large energy gap indicates a high stability of the molecule in a chemical reaction. Comparison of frontier orbitals of three protonated forms (table 8) shows that the energies of the busy frontier orbital (HOMO) are respectively -0.386, -0.384, -0.361 and -0.278, -0.280, -0.261 in the gaseous and solvated phases leading to the conclusion that the protonated compounds are more stable than the neutrals -0.231, -0.232.

Table 8 Energies of frontier orbitals in u.a

	DiuronNeutral	Diuron Protonated		
		prot(O)	prot(N ₁)	prot(N ₂)
HOMO	-0.23134 (-0.23247)	-0.38592 (-0.27787)	-0.38371 (-0.27990)	-0.36133 (-0.26136)
LUMO	-0.03674 (-0.03891)	-0.17504 (-0.06368)	-0.18361 (-0.06742)	-0.19467 (-0.06840)
ΔE	0.19460 (0.19357)	0.21088 (0.21419)	0.20677 (0.21248)	0.16666 (0.19296)

In the following figure, we have represented the frontier molecular orbitals associated in the two phases.

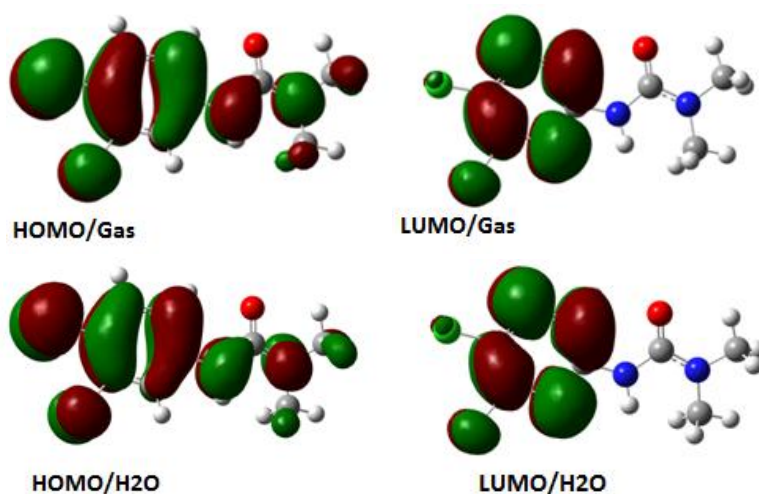


Fig. 3. Schematic representation of the frontier orbitals for Diuron

The HOMO orbitals of the compounds present a strong contribution of the fragment of dimethylurea while the two LUMO's orbitals are similar in the gas and in aqueous phases. Comparison of the difference in energy between the two frontiers orbital shows that the protonated form of the pesticide is more stable than the neutral form. The obtained molecular ions are stable compared to the energy difference between the orbital HOMO and LUMO which is of the order of 5.8eV and 5.2eV respectively for the protonated in O and N. The analysis of the results shows that the solvation leads to similar results with a decrease in the gap between the frontier orbitals in order of 0.3 eV. The values obtained for the molecular orbitals borders determine the overall indices reflecting the chemical reactivity of the studied system.

F. Global and Local Reactivity Descriptors

To determine the reactive sites of Diuron, we are interested in the local indices. Indeed, the general behavior of a molecule can be analyzed using the global reactivity parameters derived from Density Functional Theory. The vertical electronic affinity (EA) and the ionization potential (IP) can be calculated as $EA = E(N-1) - E(N)$, $IP = E(N) - E(N+1)$ where $E(N)$ is the total ground energy in the neutral N, $E(N-1)$ and $E(N+1)$ respectively the singly charged (N-1) and (N+1) configurations. The parameters are the electronic chemical potential (μ), the electronegativity (χ), hardness (η) and the global electrophilicity index (ω) which can be determined using the following equations [32–38]:

$$\begin{aligned} \mu &= -1/2 (IP - EA), \\ \eta &= (IP - EA) \\ \omega &= \mu^2 / 2\eta \end{aligned}$$

The electronic chemical potential can be associated to the escaping tendency of an electron [15]. The hardness η is correlated to the polarizability of the system [39,40]. The global electrophilicity index ω determines the possibility of chemical groups to accept electrons where higher and low values illustrate respectively the presence of good electrophiles and nucleophiles [38]. These values were used to calculate the global reactivity descriptors μ , η , ω and N that describe the molecule as a whole and permit the description of global reactivity affinities [32]. The results obtained are grouped in the table 10. The global reactivity descriptors in the aqueous phase was obtained at the B3LYP/6-311++G (d,p) level of theory.

Table 9 Global reactivity descriptors of Diuron at the B3LYP/6-311G++(d,p) level of theory in the gas phase and aqueous phase.

	I (eV)	A (eV)	η (eV)	μ (eV)	ω (eV)	N (eV)
DIURON	6.295 (6.326)	0.999 (1.059)	5.295 (5.267)	3.647 (3.692)	1.256 (1.294)	3.080 (3.049)

The results obtained are in good agreement with those reported in the literature[41]. However, to evaluate the punctual distribution of molecular reactivity, it is indispensable to estimate the descriptors of local reactivity descriptors as function of Fukui, which reproduces the part of the electron density to deform under the effect of a modification in the number of electrons in the system. The functions of Fukui f_k^+ , f_k^- , f_k^0 allow differentiation in a molecular system, the most favorable sites to accept or lose the electronic density. In a molecule with N electrons, the condensed Fukui functions for electrophilic, nucleophilic and free radical were proposed by Yang and Mortier[42] and evaluated through the following equations:

$$f_k^+ = [q_k(N + 1) - q_k(N)]$$

$$f_k^- = [q_k(N) - q_k(N - 1)]$$

$$f_k^0 = \frac{1}{2} [q_k(N - 1) - q_k(N + 1)]$$

where $q_k(N)$, $q_k(N + 1)$, $q_k(N - 1)$ are respectively the electronic population of the k atom in the neutral, anionic and cationic molecule. It has been proven previously that a large value of the index of Fukui meant responsiveness of the site for the reactions controlled by the molecular orbital borders[43]. It is essential to reveal that the Fukui function values obtained from various population schemes may provide negative values. The determination of the various parameters, in two phases, led us to the values in the following tables and figure 4.

Table 10 Local reactivity descriptors of Diuron at the B3LYP/6-311G++ (d,p) level of theory in the gas phase.

	$q_k(N)$	$q_k(N + 1)$	$q_k(N - 1)$	f_k^+	f_k^-	f_k^0	ω_k	N_k
C 1	0,17991	0,09612	0,16604	-0,08379	0,01387	-0,03496	-0,10525	0,04271
C 2	-0,22371	-0,11226	-0,00673	0,11145	-0,21698	-0,05276	0,13999	-0,66822
C 3	-0,2468	-0,10878	-0,07307	0,13802	-0,17373	-0,01785	0,17337	-0,53502
C 4	-0,09274	-0,05034	0,11803	0,0424	-0,21077	-0,08418	0,05326	-0,64909
C 5	-0,0548	-0,02653	-0,02262	0,02827	-0,03218	-0,00195	0,03551	-0,09910
C 6	-0,18572	-0,08858	-0,11512	0,09714	-0,0706	0,01327	0,12202	-0,21742
C 7	0,82467	0,41359	0,38229	-0,41108	0,44238	0,01565	-0,51636	1,36236
C 8	-0,35349	-0,17361	-0,18602	0,17988	-0,16747	0,00621	0,22595	-0,51574
C 9	-0,372	-0,18517	-0,20017	0,18683	-0,17183	0,00750	0,23468	-0,52917
N 1	-0,62289	-0,3124	-0,13065	0,31049	-0,49224	-0,09088	0,39001	-1,51592
N 2	-0,52277	-0,26179	-0,10094	0,26098	-0,42183	-0,08042	0,32782	-1,29908
O 1	-0,66626	-0,3436	-0,32344	0,32266	-0,34282	-0,01008	0,40529	-1,05576
Cl 1	0,02465	-0,00379	0,14326	-0,02844	-0,11861	-0,07353	-0,03572	-0,36527
Cl 2	0,02757	0,00265	0,06786	-0,02492	-0,04029	-0,03261	-0,03130	-0,12408
H 1	0,25754	0,12651	0,13761	-0,13103	0,11993	-0,00555	-0,16459	0,36934
H 2	0,22368	0,1052	0,12752	-0,11848	0,09616	-0,01116	-0,14882	0,29614
H 3	0,21316	0,11219	0,1183	-0,10097	0,09486	-0,00306	-0,12683	0,29213
H 4	0,39043	0,20357	0,20323	-0,18686	0,1872	0,00017	-0,23472	0,57651
H 5	0,18171	0,09166	0,11733	-0,09005	0,06438	-0,01284	-0,11311	0,19827
H 6	0,18605	0,094	0,11348	-0,09205	0,07257	-0,00974	-0,11562	0,22349
H 7	0,23833	0,11318	0,12517	-0,12515	0,11316	-0,00599	-0,15720	0,34849
H 8	0,2131	0,10851	0,12038	-0,10459	0,09272	-0,00594	-0,13138	0,28554
H 9	0,18845	0,10055	0,11205	-0,0879	0,0764	-0,00575	-0,11041	0,23528
H 10	0,19192	0,09914	0,10621	-0,09278	0,08571	-0,00354	-0,11654	0,26395

It is interesting to note, according to the results, that the most reactive positions of Diuron are located on N1, N2 and O1. In fact the values of ω_k obtained are respectively 0.39, 0.33 and 0.41 confirming that the most favourable site for an electrophilic attack is the oxygen of the carbonyl group. In regards to nucleophilic attack, the results give us 1.36, 1.52 for N1 and N2 showing that the most likely sites are C7 and N1 on Diuron and would cause a substitution of the hydrogen atom. The same approach was conducted for the study in an aqueous medium. The results are grouped in table 11.

Table 11 Local reactivity descriptors of Diuron at the B3LYP/6-311G++ (d,p) level of theory in the aqueous phase.

	$q_k(N)$	$q_k(N + 1)$	$q_k(N - 1)$	f_k^+	f_k^-	f_k^0	ω_k	N_k
C 1	0,18433	0,08366	0,16060	-0,10067	0,02373	-0,03847	-0,13028	0,07235
C 2	-0,22769	-0,10058	0,00034	0,12711	-0,22803	-0,05046	0,16449	-0,69524
C 3	-0,24229	-0,06007	-0,03611	0,18222	-0,20618	-0,01198	0,23582	-0,62862
C 4	-0,09798	-0,06577	0,12520	0,03221	-0,22318	-0,09548	0,04168	-0,68045
C 5	-0,05724	-0,00011	-0,03979	0,05713	-0,01745	0,01984	0,07393	-0,05320
C 6	-0,19257	-0,03056	-0,1189	0,16201	-0,07367	0,04417	0,20966	-0,22461
C 7	0,82661	0,41272	0,38267	-0,41389	0,44394	0,01503	-0,53563	1,35352
C 8	-0,35471	-0,17707	-0,18477	0,17764	-0,16994	0,00385	0,22989	-0,51813
C 9	-0,37757	-0,18679	-0,20034	0,19078	-0,17723	0,00678	0,24689	-0,54035
N 1	-0,62108	-0,31496	-0,09176	0,30612	-0,52932	-0,11160	0,39616	-1,61383
N 2	-0,50408	-0,25653	-0,08879	0,24755	-0,41529	-0,08387	0,32036	-1,26617
O 1	-0,72204	-0,36788	-0,35092	0,35416	-0,37112	-0,00848	0,45833	-1,13150
Cl 1	0,00834	-0,02343	0,10293	-0,03177	-0,09459	-0,06318	-0,04111	-0,28839
Cl 2	0,01592	-0,02433	0,03924	-0,04025	-0,02332	-0,03178	-0,05209	-0,07110
H 1	0,24966	0,10939	0,13229	-0,14027	0,11737	-0,01145	-0,18153	0,35785
H 2	0,23195	0,09550	0,12843	-0,13645	0,10352	-0,01647	-0,17658	0,31562
H 3	0,23275	0,09778	0,12605	-0,13497	0,10670	-0,01414	-0,17467	0,32531
H 4	0,41089	0,20060	0,21363	-0,21029	0,19726	-0,00652	-0,27214	0,60142
H 5	0,19196	0,09384	0,11772	-0,09812	0,07424	-0,01194	-0,12698	0,22635
H 6	0,19582	0,09599	0,11496	-0,09983	0,08086	-0,00949	-0,12919	0,24653
H 7	0,22558	0,11208	0,11802	-0,11350	0,10756	-0,00297	-0,14688	0,32794
H 8	0,21944	0,10754	0,11898	-0,11190	0,10046	-0,00572	-0,14481	0,30629
H 9	0,1985	0,09728	0,11770	-0,10122	0,08080	-0,01021	-0,13099	0,24635
H 10	0,20551	0,10172	0,11264	-0,10379	0,09287	-0,00546	-0,13432	0,28315

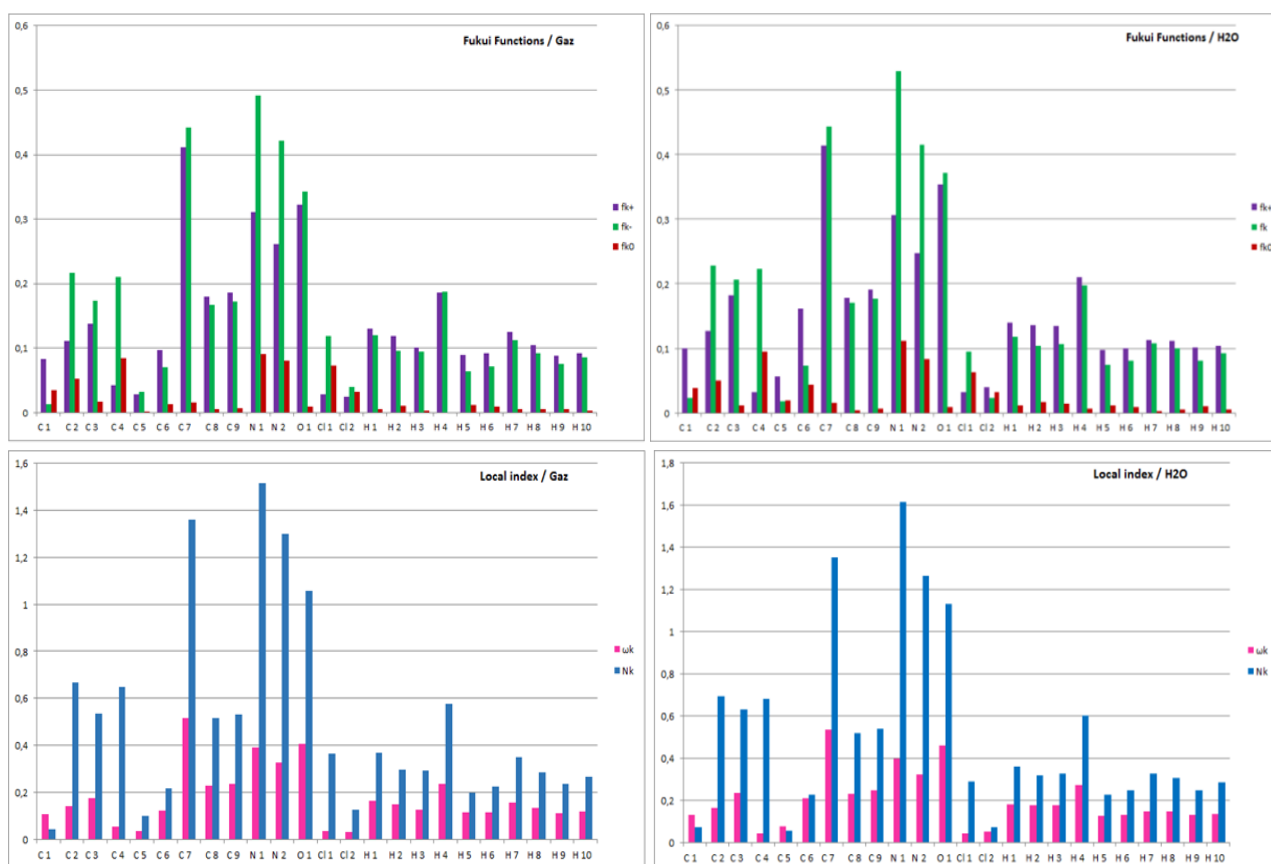


Fig. 4. Values of the Fukui function for Diuron

The analysis of the results in aqueous medium lead to the same conclusions as those obtained in the gas phase. From all the results detailed above for Diuron, we can conclude that the electrophilic attack protonation will be most preferentially at the level of the urea, more particularly on the oxygen of the carbonyl and the protonation would produce of course the elimination of the fragment of dimethylurea.

G. IR Study

A frequency analysis was applied to the optimized geometries of the neutral pesticide and its protonated forms, in gaseous and aqueous phases (values in parenthesis), to verify that the stationary points correspond to the minimum of the potential energy surface. In all cases, the frequency values were positive and no imaginary frequency was obtained. Thus, it could be identified strong stretching vibrations of the carbonyl bond at 1701cm^{-1} (1648cm^{-1}), stretching N-H vibrations at 3578cm^{-1} (3564cm^{-1}) while N-C-N symmetric stretching vibrations were observed at 1021cm^{-1} (1023cm^{-1}). These values are in good agreement with those reported in the literature for phenylurea compounds[44].

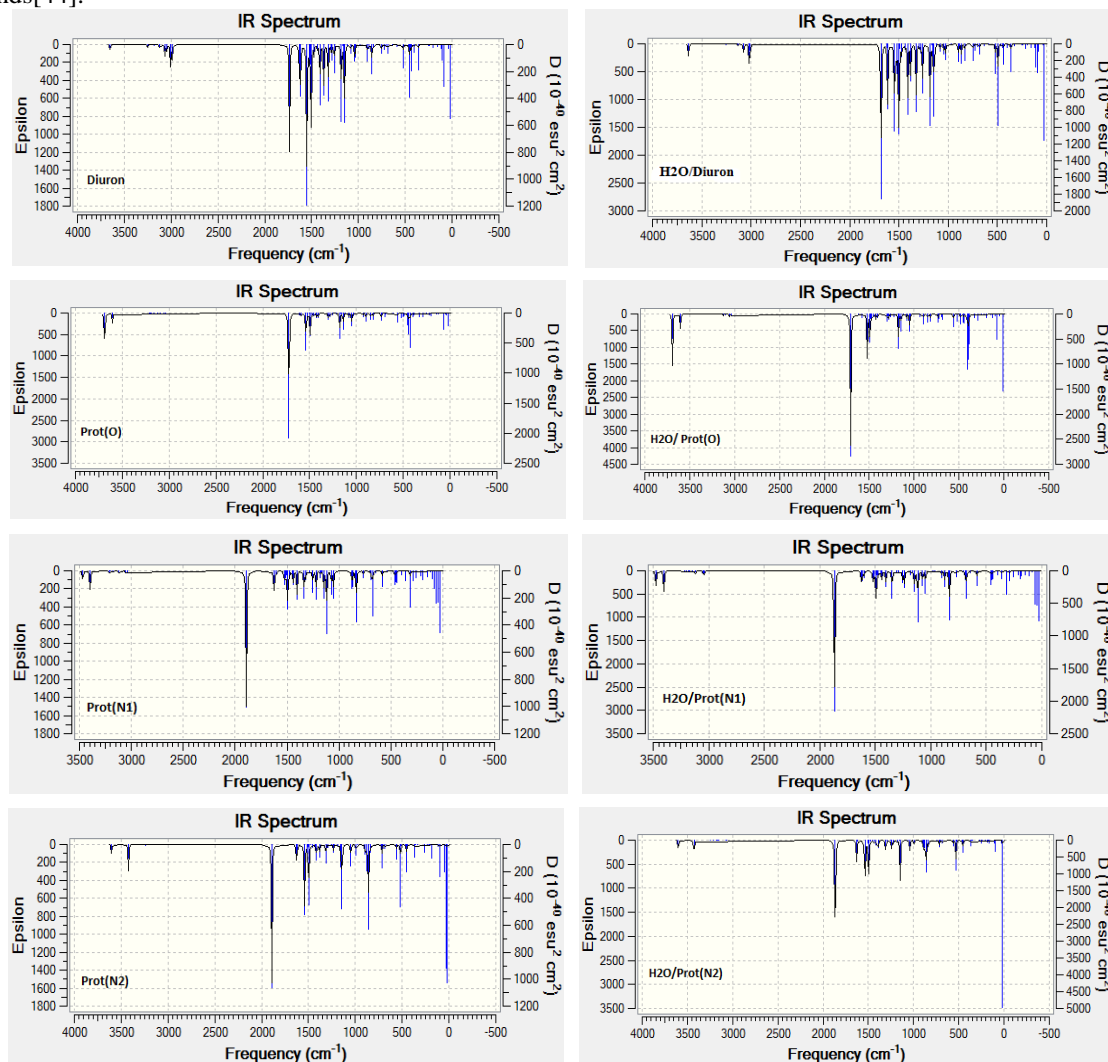


Fig.5. IR spectra of the neutral and protonated isomers of Diuron in gaseous and aqueous phases

The spectroscopic study of Diuron show us the absorption bands in gaseous and aqueous phases: 437cm^{-1} (432cm^{-1}) bands characterizing the absorption of benzene ring cycle; 1599cm^{-1} (1595cm^{-1}) correspond to the absorption of the C=C bonds for different isomers, 3100cm^{-1} and 3057cm^{-1} (3104cm^{-1} and 3068cm^{-1}) determine the absorption of the C-H for the methyl group; 3578cm^{-1} (3564cm^{-1}) and 1701cm^{-1} (1648cm^{-1}) correspond to the absorptions of the N-H and the C=O bonds respectively. It may be noted the appearance of the frequencies 3449cm^{-1} , 3246cm^{-1} and 3206cm^{-1} which means respectively the O-H bond for the protonated at the site of the carbonyl, the N-H bond for the protonated on N1 and N2. In aqueous solution, it has a displacement of absorption bands. For Diuron and its three protonated forms, the results show a shift of absorption bands. Indeed, in the case of the different forms protonated on O, N1 and N2, we get respectively 1818cm^{-1} for C=O, 3463cm^{-1} for N-H, 3264cm^{-1} and 3289cm^{-1} for NH^+ , 3549cm^{-1} for the binding OH^+ .

IV. CONCLUSION

The theoretical data using DFT density functional theory helped to verify the stability of the protonated forms of Diuron by the determination of energies and reveal that the protonation does not affect the geometry. However, these calculations have shown that the energies of formation of all monoprotonated compounds are very close and concluded

that protonation on the carbonyl group was the most favourable. Frontier orbital analysis has shown that the protonated form is more stable by the formation of a hydrogen bond. The analysis of the chemical reactivity of Diuron herbicide in the gas phase and aqueous phase employing global and local reactivity IP, EA, μ , η , ω , N indicates that the electrophilic attack will be most preferentially at the level of the urea, more particularly on the oxygen of the carbonyl. The frequencies of the internal modes calculated for the neutral form and various protonated forms showed a difference of spectra that can be used in a later comparison with experimental results.

ACKNOWLEDGEMENTS

We thank AMCT for providing Gaussian03

REFERENCES

- [1] Sjollega SB, MartínezGarcía G, van der Geest HG, Kraak MHS, Booij P, Vethaak AD, et al. Hazard and risk of herbicides for marine microalgae. *Environ Pollut* 2014;187:106–11. doi:10.1016/j.envpol.2013.12.019.
- [2] Quintás G, Morales-Noé A, Parrilla C, Garrigues S, de la Guardia M. Fourier transform infrared determination of Fluometuron in pesticide formulations. *Vib Spectrosc* 2003;31:63–9. doi:10.1016/S0924-2031(02)00067-X.
- [3] Cardoso APF, Ihlaseh Catalano SM, da Rocha MS, Nascimento e Pontes MG, de Camargo JLV, de Oliveira MLCS. Dose–response of diuron [3-(3,4-dichlorophenyl)-1,1-dimethylurea] in the urothelial mucosa of Wistar rats. *Toxicology* 2013;312:1–5. doi:10.1016/j.tox.2013.07.007.
- [4] Quintás G, Armenta S, Morales-Noé A, Garrigues S, de la Guardia M. Simultaneous determination of Folpet and Metalaxyl in pesticide formulations by flow injection Fourier transform infrared spectrometry. *Anal Chim Acta* 2003;480:11–21. doi:10.1016/S0003-2670(02)01596-9.
- [5] Nascimento MG, de Oliveira MLCS, Lima AS, de Camargo JLV. Effects of Diuron [3-(3,4-dichlorophenyl)-1,1-dimethylurea] on the urinary bladder of male Wistar rats. *Toxicology* 2006;224:66–73. doi:10.1016/j.tox.2006.04.029.
- [6] Gläßgen WE, Komossa D, Bohnenkämper O, Haas M, Hertkorn N, May RG, et al. Metabolism of the Herbicide Isoproturon in Wheat and Soybean Cell Suspension Cultures. *PesticBiochemPhysiol* 1999;63:97–113. doi:10.1006/pest.1999.2394.
- [7] Field JA, Reed RL, Sawyer TE, Griffith SM, Wigington PJ. Diuron occurrence and distribution in soil and surface and ground water associated with grass seed production. *J Environ Qual* 2003;32:171–9.
- [8] Vroumsia T, Steiman R, Seigle-Murandi F, Benoit-Guyod JL, Khadrani A. Biodegradation of three substituted phenylurea herbicides (chlortoluron, diuron, and isoproturon) by soil fungi. A comparative study. *Chemosphere* 1996;33:2045–56.
- [9] Freitas JS, Kupsco A, Diamante G, Felicio AA, Almeida EA, Schlenk D. Influence of Temperature on the Thyroidogenic Effects of Diuron and Its Metabolite 3,4-DCA in Tadpoles of the American Bullfrog (*Lithobates catesbeianus*). *Environ Sci Technol* 2016;50:13095–104. doi:10.1021/acs.est.6b04076.
- [10] Amine-Khodja A, Boulkamh A, Boule P. Photochemical behaviour of phenylurea herbicides. *Photochem Photobiol Sci* 2004;3:145–56. doi:10.1039/B307968F.
- [11] Moncada A, Environmental Fate of Diuron - diuron.pdf n.d.
- [12] Chen W-H, Young TM. Influence of Nitrogen Source on NDMA Formation during Chlorination of Diuron. *Water Res* 2009;43:3047–56. doi:10.1016/j.watres.2009.04.020.
- [13] Feng J, Zheng Z, Sun Y, Luan J, Wang Z, Wang L, et al. Degradation of diuron in aqueous solution by dielectric barrier discharge. *J Hazard Mater* 2008;154:1081–9. doi:10.1016/j.jhazmat.2007.11.013.
- [14] Pei K, Su M, Chen L, Li F, Zheng X. Resonance Raman spectroscopy and theoretical study on the photodissociation dynamics of diuron in S2 state. *J Raman Spectrosc* 2012;43:1969–74. doi:10.1002/jrs.4117.
- [15] Parr RG, Donnelly RA, Levy M, Palke WE. Electronegativity: The density functional viewpoint. *J Chem Phys* 1978;68:3801–7. doi:10.1063/1.436185.
- [16] Ziegler T. Approximate density functional theory as a practical tool in molecular energetics and dynamics. *Chem Rev* 1991;91:651–67. doi:10.1021/cr00005a001.
- [17] Bartolotti LJ, Flurchick K. An Introduction to Density Functional Theory. In: Lipkowitz KB, Boyd DB, editors. *Rev. Comput. Chem.*, John Wiley & Sons, Inc.; 1996, p. 187–216.
- [18] Baerends EJ, Gritsenko OV. A Quantum Chemical View of Density Functional Theory. *J Phys Chem A* 1997;101:5383–403. doi:10.1021/jp9703768.
- [19] Becke null. Density-functional exchange-energy approximation with correct asymptotic behavior. *Phys Rev Gen Phys* 1988;38:3098–100.
- [20] van Leeuwen R, Baerends EJ. Exchange-correlation potential with correct asymptotic behavior. *Phys Rev A* 1994;49:2421–31. doi:10.1103/PhysRevA.49.2421.
- [21] Becke AD. Density- functional thermochemistry. III. The role of exact exchange. *J Chem Phys* 1993;98:5648–52. doi:10.1063/1.464913.
- [22] Boese AD. Density Functional Theory and Hydrogen Bonds: Are We There Yet? *ChemPhysChem* 2015;16:978–85. doi:10.1002/cphc.201402786.
- [23] Gaussian 09, Revision A.02 <http://gaussian.com>.
- [24] Kanawati B, Harir M, Schmitt-Kopplin P. Exploring rearrangements along the fragmentation pathways of diuron anion: A combined experimental and computational investigation. *Int J Mass Spectrom* 2009;288:6–15. doi:10.1016/j.ijms.2009.07.010.

- [25] Alcolea Palafox M, Rastogi VK. Quantum chemical predictions of the vibrational spectra of polyatomic molecules.: The uracil molecule and two derivatives. *Spectrochim Acta A Mol Biomol Spectrosc* 2002;58:411–40. doi:10.1016/S1386-1425(01)00509-1.
- [26] Dennington R, Keith T, Millam J, Eppinnett K, Lee Hovell W, Gilliland R, GaussView, Version 3.0.9, Semichem Inc., Shawnee Mission, KS, 2003
- [27] Cammi R, Tomasi J. Quantum Cluster Theory for the Polarizable Continuum Model (PCM). In: Leszczynski J, editor. *Handb. Comput. Chem.*, Springer Netherlands; 2012, p. 1043–66. doi:10.1007/978-94-007-0711-5_28.
- [28] Li H, Fedorov DG, Nagata T, Kitaura K, Jensen JH, Gordon MS. Energy gradients in combined fragment molecular orbital and polarizable continuum model (FMO/PCM) calculation. *J Comput Chem* 2010;31:778–90. doi:10.1002/jcc.21363.
- [29] Vroumsia T, Steiman R, Seigle-Murandi F, Benoit-Guyod J-L, Khadrani A, Groupe pour l'Étude du Devenir des Xénobiotiques dans l'Environnement (GEDEXE). Biodegradation of three substituted phenylurea herbicides (chlortoluron, diuron, and isoproturon) by soil fungi. A comparative study. *Chemosphere* 1996;33:2045–56. doi:10.1016/0045-6535(96)00318-9.
- [30] Vrielynck L, Lapouge C, Marquis S, Kister J, Dupuy N. Theoretical and experimental vibrational study of phenylurea: structure, solvent effect and inclusion process with the β -cyclodextrin in the solid state. *Spectrochim Acta A Mol Biomol Spectrosc* 2004;60:2553–9. doi:10.1016/j.saa.2003.12.035.
- [31] Mendoza-Huizar LH. Chemical Reactivity of Isoproturon, Diuron, Linuron, and Chlorotoluron Herbicides in Aqueous Phase: A Theoretical Quantum Study Employing Global and Local Reactivity Descriptors. *J Chem* 2015;2015:e751527. doi:10.1155/2015/751527.
- [32] Gázquez JL. Perspectives on the density functional theory of chemical reactivity. *J Mex Chem Soc* 2008;52:3–10.
- [33] Geerlings P, De Proft F, Langenaeker W. Conceptual Density Functional Theory. *Chem Rev* 2003;103:1793–874. doi:10.1021/cr990029p.
- [34] Chermette H. Chemical reactivity indexes in density functional theory. *J Comput Chem* 1999;20:129–54. doi:10.1002/(SICI)1096-987X(19990115)20:1<129::AID-JCC13>3.0.CO;2-A.
- [35] Ayers PW, Anderson JSM, Bartolotti LJ. Perturbative perspectives on the chemical reaction prediction problem. *Int J Quantum Chem* 2005;101:520–34. doi:10.1002/qua.20307.
- [36] Chattaraj PK, Sarkar U, Roy DR. Electrophilicity Index. *Chem Rev* 2006;106:2065–91. doi:10.1021/cr040109f.
- [37] LIU S-B. Conceptual Density Functional Theory and Some Recent Developments. *Acta Phys-Chim Sin* 2009;25:590–600.
- [38] Parr RG, Szentpály L v., Liu S. Electrophilicity Index. *J Am Chem Soc* 1999;121:1922–4. doi:10.1021/ja983494x.
- [39] Parr RG, Pearson RG. Absolute hardness: companion parameter to absolute electronegativity. *J Am Chem Soc* 1983;105:7512–6. doi:10.1021/ja00364a005.
- [40] Pearson RG. Recent advances in the concept of hard and soft acids and bases. *J Chem Educ* 1987;64:561. doi:10.1021/ed064p561.
- [41] Otero N, Karamanis P, El-Kelany KE, Rerat M, Maschio L, Civalleri B, et al. Exploring the Linear Optical Properties of Borazine (B₃N₃) Doped Graphenes. 0D Flakes vs 2D Sheets. *J Phys Chem C* 2017;121:709–722. doi:10.1021/acs.jpcc.6b10837.
- [42] Yang W, Mortier WJ. The use of global and local molecular parameters for the analysis of the gas-phase basicity of amines. *J Am Chem Soc* 1986;108:5708–11. doi:10.1021/ja00279a008.
- [43] Salah M, Komiha N, Kabbaj OK, Ghailane R, Marakchi K. Computational study of the 1,3-dipolar cycloaddition between methyl 2-trifluorobutynoate and substituted azides in terms of reactivity indices and activation parameters. *J Mol Graph Model* 2017;73:143–51. doi:10.1016/j.jmgm.2017.02.017.
- [44] Gunasekaran S, Natarajan RK, Syamala D, Rathikha R. Normal coordinate analysis of urea meta nitro benzoic acid crystal. *IJPAP Vol4404 April* 2006.